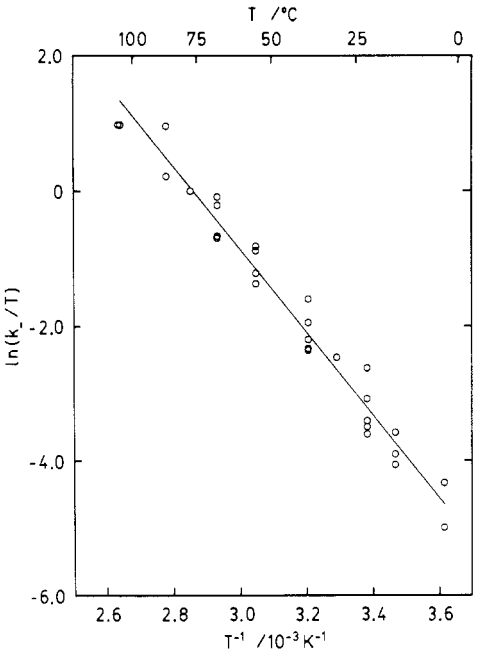

Figure 10. Temperature dependence of the rate coefficient k_- for dissociation of the dimer $H_4Si_2O_7^{2-}$.

for single species (other than the monomer) except at high pH, where the additional complication of unknown degrees of multiple deprotonation of the various silicate species arises. Nevertheless, for solutions with M^+:Si^{IV} = 1.0:1, it is possible to estimate roughly the rate coefficient k_- for cleavage of the dimer $H_4Si_2O_7^{2-}$ ($^1Q^1_2$) from eq 5, in which k_+ ($=\tau^{-1}/[^*Q^0]$) is the first-order rate coefficient for dimerization and p_m and p_d are the integrated areas of the monomer and dimer resonances, respectively.

$$k_- = k_+[^*Q^0][^1Q^0]/[^1Q^1_2] = \tau^{-1}[^1Q^0]/[^1Q^1_2] = 2\tau^{-1}p_m/p_d \quad (5)$$

Figure 10 summarizes the available data for solutions with Na^+:Si^{IV} = 1.0:1 in terms of eq 1 and 5. The k_- values refer to widely differing media and carry an uncertainty of about ±20% but are adequately represented by $\Delta H_-^* = 51.0 \pm 1.7$ kJ mol^{-1} and $\Delta S_-^* = -51.8 \pm 5.4$ J K^{-1} mol^{-1}, which give $k_- = 14$ s^{-1} at 298.2 K.

Conclusion. Our findings demonstrate that temperature-dependent line broadening in ^{29}Si spectra of aqueous silicate solutions is indeed the result of Si–Si chemical exchange at rates within the NMR time frame (roughly 1 s to 0.1 ms, from ambient temperature to about 150 °C). For readily cyclizable species such as the acyclic trimer, cyclization is more rapid than intermolecular condensation. For M^+:Si^{IV} = 1.0:1, at which each Si normally carries one $-O^-$ group, the rate of intermolecular condensation is essentially the same for all Si centers that are not easily cyclized, implying that there is a common vehicle of Si exchange which is probably an active forrm of the monomer. At higher pH levels, i.e., at M^+:Si^{IV} ratios higher than 1.0:1, substantial fractions of the silicate centers carry two $-O^-$ groups and are relatively unreactive, resulting in a decrease in both polymerization and cyclization rates and a shift in the equilibrium distribution of silicate species toward the monomer and low-molecular-mass oligomers.

Most of the controversy that has arisen over the origin of the temperature-dependent line broadening of aqueous silicates has stemmed from failure to consider the effect of pH or of the leaching of line-broadening contaminants from glass sample tubes. When deprotonation equilibria are taken into account, line-broadening analyses and selective inversion-recovery experiments are seen to be in agreement.

Finally, there is evidence for a small contribution to ^{29}Si line widths from Si–M nuclear dipole–dipole relaxation, but this effect is significant only at temperatures below 20 °C and/or very high pH, i.e., when Si–Si exchange broadening is negligible.

Acknowledgment. We thank Prof. R. K. Harris for discussions, the Alberta Oil Sands Technology and Research Authority for a scholarship (to S.D.K.), and The University of Calgary Research Grants Committee and the Natural Sciences and Engineering Research Council of Canada for financial assistance.

Registry No. Si, 7440-21-3; $Si(OH)_4$, 10193-36-9; $H_4Si_2O_7^{2-}$, 51931-86-3; SiO_2, 7631-86-9.

Supplementary Material Available: Tables of line widths as functions of temperature and alkalinity and (for the monomer–dimer equilibrium) integrated peak areas and rate coefficients (3 pages). Ordering information is given on any current masthead page.

Contribution from the Department of Chemistry, University of Washington, Seattle, Washington 98195

The $FeBr_2$–Br_2–H_2O–HBr System. Iron(III) Bromide Hydrate in the Vapor Phase

N. W. Gregory

Received May 18, 1988

Absorbances of vapors generated by $FeBr_2$–Br_2–HBr–H_2O mixtures at temperatures between 400 and 700 K have been measured in the wavelength range 300–480 nm. Evidence is found for substantial concentrations of a hydrate in the vapor phase, along with Fe_2Br_6(g) and $FeBr_3$(g). $Fe(H_2O)Br_3$(g) is assumed to be the dominant hydrate vapor molecule. Molar absorptivities at various wavelengths and thermodynamic constants are derived. For $Fe(H_2O)Br_3$(g) at 500 K, $\Delta H^\circ = -508$ kJ mol^{-1} and S° = 502 J K^{-1} mol^{-1}.

Introduction

The recent finding of iron(III) chloride hydrate molecules[1,2] in the vapor phase has motivated a search for similar hydrate molecules in the iron bromide system. In the presence of solid iron(II) bromide, the concentrations of iron(III) bromide dimer, Fe_2Br_6(g), and monomer, $FeBr_3$(g), are fixed by the concentration of bromine, Br_2(g). Equilibrium reactions 1 and 2 have been studied in previous work.[3-6] If the addition of water vapor to a mixture of solid iron(II) bromide and bromine forms a volatile hydrate, as in reaction 3, then the total concentration of iron(III) bromide molecules in the vapor, and hence the vapor phase absorbance, should be enhanced.

$$2FeBr_2(s) + Br_2(g) = Fe_2Br_6(g) \quad (1)$$

$$FeBr_2(s) + 0.5Br_2(g) = FeBr_3(g) \quad (2)$$

$$FeBr_2(s) + 0.5Br_2(g) + H_2O(g) = Fe(H_2O)Br_3(g) \quad (3)$$

(1) Gregory, N. W. *Inorg. Chem.* **1983**, *22*, 3750–3754.
(2) Rustad, D. S.; Gregory, N. W. *Inorg. Chem.* **1988**, *27*, 2840–2844.
(3) Gregory, N. W.; Thackrey, B. A. *J. Am. Chem. Soc.* **1955**, *72*, 3176–3178.
(4) MacLaren, R. O.; Gregory, N. W. *J. Phys. Chem.* **1955**, *59*, 184–186.
(5) Gregory, N. W.; MacLaren, R. O. *J. Phys. Chem.* **1955**, *59*, 110–113.
(6) Gregory, N. W. *J. Phys. Chem.* **1977**, *81*, 1857–1860.

0020-1669/88/1327-4264$01.50/0

Table I. Cell Dimensions, Amounts of Reactants,[a] and Intersect Temperatures, $T_{1,2}$, for Ranges 1 and 2 for Various Samples

sample	cell length, cm	cell vol, cm^3	10^3C_b(400 K), mol L^{-1}	$10^2C_0(H_2O)$, mol L^{-1}	10^2C_0(HBr), mol L^{-1}	10^5C_0(Fe), mol L^{-1} anal.	10^5C_0(Fe), mol L^{-1} spec	$T_{1,2}$, K
1	5	15.5	0.737	(0.808)	1.55	6.58		
2	5	15.4	0.306	(0.617)	1.65	7.18		
3	1	3.99	2.13	1.401	1.02	56.09		499
4	2	6.37	6.40	0.303	1.57	11.35	11.30	456
5	5	15.4	0.694	1.805	0.487	32.6		490
6	10	29.8	1.63	0.936	0.510	3.92	4.09	476
7	1	3.42	11.75	1.632	0.573		2.50	522
8	5	15.9	0.741	1.758	0.882	5.58	5.82	491

[a] C_b(400 K) = concentration calculated from observed bromine absorbance at ca. 400 K. Other C_0 values = moles introduced/cell volume.

A spectrophotometric study of vapors generated by $FeBr_2$–Br_2–H_2O–HBr mixtures is now reported. Hydrogen bromide was introduced to reduce the tendency for formation of iron oxides and/or oxybromides. The UV–visible absorption vapor spectra show absorbances greater than expected from the concentrations of dimer, $Fe_2Br_6(g)$, monomer, $FeBr_3(g)$, and bromine. The extra absorbance depends on the concentrations of bromine and water in the way predicted for reaction 3. Equilibrium constants and thermodynamic properties have been derived on the basis of the assumption that the dominant reactions involving the hydrate are reactions 3 and 4. Results are compared with the earlier study of the chloride system.[2]

$$0.5Fe_2Br_6(g) + H_2O(g) = Fe(H_2O)Br_3(g) \qquad (4)$$

Experimental Section

Vapor-phase absorbances of eight different samples at various temperatures were recorded over the range 300–480 nm with a Cary 14H Spectrophotometer. Samples were contained in sealed cylindrical quartz absorption cells, 20 mm o.d., with various path lengths. The reactants were introduced into the cells through side arms, 6 mm o.d., attached at the centers of the cells and connected to a vacuum system. Except for samples 1 and 2, which had graded seals attached to Pyrex side arms, samples were prepared and isolated in all-quartz systems.

First, analytical grade iron (Baker and Adamson Standardization wire, 99.90%), placed in an extension of a side arm, was reacted with dry bromine (Bakers Analyzed Reagent), forming a mixture of iron(II) bromide, $FeBr_2$, and iron(III) bromide, $FeBr_3$. When the mixture was heated in vacuum, $FeBr_3$ decomposed to bromine and $FeBr_2$. A small amount of $FeBr_2$ was then sublimed in vacuum into the cell. An amount of bromine, sufficient to generate iron(III) bromide vapors by reactions 1 and 2, was then condensed into the cell (cooled with liquid nitrogen), along with dry hydrogen bromide (Matheson). The amount of HBr was calculated from a measured pressure in a known volume. Finally a measured amount of water was condensed in the cell. For samples 1 and 2, the quantity of water vapor was calculated from a measured pressure (ca. 10 Torr) in a known volume. For samples 3–8 a sample of water vapor, initially equilibrated with an ice–liquid water mixture, was isolated in a known volume (at room temperature); the amount was calculated from the ideal gas law by using the triple-point pressure. The mixture in the cell was finally isolated by sealing off the quartz side arm with a flame.

With a sample around 400 K the bromine absorbance was measured at several wavelengths and the concentration of bromine calculated by using molar absorptivities determined by Passchier.[7] After completion of all absorbance measurements the tip of the cell side arm was cracked off. The cell contents were dissolved in 2% HNO_3 solution, and the amount of iron was determined by using an ICP emission spectrometer (Model 955 Plasmo Atomcomp). The cell volume was determined by comparison of the mass of the empty cell and the cell filled with water. Amounts of each reactant are listed in Table I.

For samples 1 and 2, the absorbance of the vapor phase generated by the $FeBr_2$–Br_2–HBr mixtures was measured before addition of water and compared with observations in earlier studies in which HBr had not been introduced. Within experimental uncertainty, no difference was observed. It was necessary to reattach these cells to the vacuum line and open the tips to introduce water. The technique has been described previously.[2] The absorbances observed for samples 1 and 2 were not compatible with those from samples 3–8 until it was assumed that small amounts of water, in addition to the measured quantities, entered the cells during the reattachment procedure. Adjusted concentrations, increased by ca. 20% over the measured quantities and shown in parentheses in Table I, brought results for these samples into agreement. Rather than discarding the observed absorbances for 1 and 2, results based on the adjusted concentrations of water have been included in the overall analysis of data.

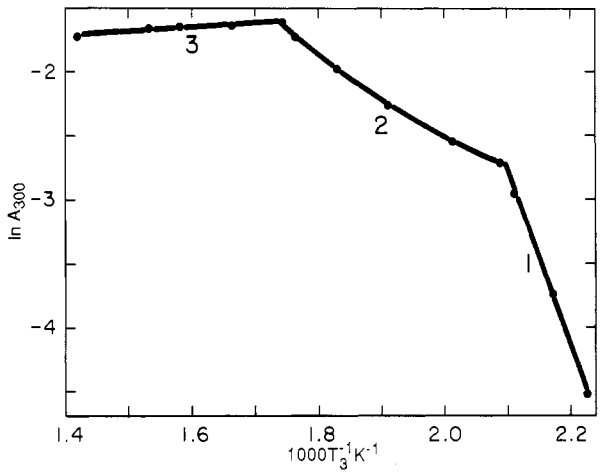

Figure 1. Values of ln A_{300} for sample 6 at various temperatures, showing the different behavior in ranges 1, 2, and 3.

The temperatures at the surface of the center of the cell, T_1, at the cell windows, T_2, and at the tip of the side arm, T_3, were measured with calibrated chromel–alumel thermocouples. When a condensed phase was present, T_1 and T_2 were kept higher than T_3 to avoid formation of deposits on the windows. The cell and side arm, respectively, were heated by separately controlled electric furnaces.[8] Values of T_1 and T_3 are listed in Table II (supplementary material).

Results and Discussion

Absorbance at 300 nm. The molar absorptivity of bromine at 300 nm, and its contribution to the total absorbance, is very small.[7] Hence the absorbance at 300 nm, A_{300}, is contributed primarily by iron bromide vapor, and observations at this wavelength were examined first. For samples 4, 6, 7, and 8 the variation of A_{300} with temperature showed three distinct ranges of behavior; a typical plot is shown in Figure 1. In range 1, a condensed hydrate phase (a liquid phase was visible at room temperature in some cases) is believed present; the absorbance in range 1 increases rapidly as the temperature is increased. In range 2, $FeBr_2(s)$ is believed the only condensed phase present, and in range 3, the iron bromide appears to have vaporized completely, as Fe_2Br_6, $FeBr_3$, and hydrate vapor molecules. The contribution of the vapor of iron(II) bromide is negligible in all ranges.[4,5] For the other samples, the amounts of the reactants were such that the absorbance could be measured only in one or two of the three ranges.

As will be shown, the absorbance in range 2 depends on the concentrations of bromine and water vapor, in the way expected if controlled by equilibrium reactions 1, 2, and 3. The total absorbance was assumed to be the sum, eq 5, of the absorbances

$$A_{300} = \epsilon_{300,b}C_b + \epsilon_{300,h}C_h + \epsilon_{300,d}C_d + \epsilon_{300,m}C_m \qquad (5)$$

of bromine, $A_{300,b} = \epsilon_{300,b}C_b$, a hydrate molecule, $A_{300,h} = \epsilon_{300,h}C_h$,

(7) Passchier, A. A. Ph.D. Thesis, University of Washington, Seattle, WA, 1968.

(8) Hilden, D. L. Ph.D. Thesis, University of Washington, Seattle, WA, 1971.

Fe_2Br_6, $A_{300,d} = \epsilon_{300,d}C_d$, and $FeBr_3$, $A_{300,m} = \epsilon_{300,m}C_m$. In these expressions ϵ_{300} represents the molar absorptivity and C represents the concentration of the component identified by the subscript. The small contribution of bromine was calculated from C_b and $\epsilon_{300,b}$.[7] C_m is also small in range 2 and was calculated from C_b and the equilibrium constant for reaction 2, $K_2 = C_m(RT_1/C_b)^{0.5}$. Values of K_2 were calculated from eq 6.[5] $\epsilon_{300,m}$ was taken as 2570

$$\ln K_2 = -12413/T_3 + 12.501 \quad (6)$$

M^{-1} cm^{-1}.[6] The contributions of monomer and bromine were subtracted from A_{300} to derive $A_{300,dh}$, assumed to be the contribution of dimer and hydrate molecules.

For equilibrium 1, $K_1 = C_d/C_b$ and $\epsilon_{300,d}C_d = \epsilon_{300,d}K_1C_b$. If eq 3 is assumed, $K_3 = C_h/C_w(C_bRT_1)^{0.5}$ and $\epsilon_{300,h}C_h = \epsilon_{300,h}K_3C_w(C_bRT_1)^{0.5}$; C_w represents the concentration of water. Equation 5 may now be written as eq 7.

$$A_{300,dh}/C_w(C_b)^{0.5} = \epsilon_{300,h}K_3(RT_1)^{0.5} + \epsilon_{300,d}K_1(C_b)^{0.5}/C_w = Y \quad (7)$$

Calculation of Equilibrium Concentrations of Bromine and Water Vapor. Amounts of bromine and water were, in all cases, large compared to the amount of iron bromide. However, to derive values of C_b and C_w for each equilibrium mixture, allowance was made for formation of iron(III) bromide molecules. As shown in the following analysis of results, at temperatures at which the bromine absorbance, and hence the concentration of free bromine, was measured, ca. 400 K, $FeBr_2$ is believed to have been converted to a condensed iron(III) bromide hydrate phase. Hence the total concentration of bromine in excess over that in the $FeBr_2$ originally introduced, $C_b(t)$, was taken as the measured concentration at 400 K, listed in Table I, plus half of the C_0 of Fe. To allow for bromine consumed by formation of iron(III) bromide vapor molecules, C_b in each equilibrium mixture was taken as $C_b(t) - C_d - 0.5(C_h + C_m)$. C_b was derived by iteration. The uncorrected values of $C_b(t)$ were used to derive trial values of C_d, C_h, and C_m. These were used to correct $C_b(t)$, and the process was repeated. No significant change was observed after the second iteration. A similar correction to C_w, to allow for formation of hydrate molecules, was less than 1%. Derived values of C_b and C_w for each equilibrium mixture are listed in Table II (supplementary material).

Partial pressures of Br_2 and H_2O were assumed to be uniform throughout the cell. Only a small percentage of the cell volume, the end of the side arm, was at T_3; however with a condensed phase present, the concentrations of iron bromide vapors are fixed by equilibrium with the condensed phase at T_3. Vapor absorbances are measured at T_1, however. To approximate a correction for the temperature difference it was assumed, for each iron(III) bromide molecule, that $C(\text{at } T_1) = C(\text{at } T_3)\ (T_3/T_1)^{0.5}$. This correction was small, <3%.

Correlation of Absorbance Data with the Concentrations of Water and Bromine Vapor. From eq 7, a value of Y was derived from each observed absorbance in range 2. To facilitate interpolation so as to compare data from the various samples at the same temperature, the temperature dependence of Y for each sample was fit by least-squares techniques to an empirical equation of the form $Y = a + b/T + c/T^2 + d/T^3$. Values of Y were then calculated at each of four temperatures: 510, 530, 550, and 570 K. With temperature as a parameter, Y is shown as a function of $(C_b)^{0.5}/C_w$ in Figure 2a. If eq 7 is valid, i.e. assuming reactions 1, 2, and 3, the observed linear relationship is expected. Values of $\epsilon_{300,h}K_3$, derived from the intercepts, and values of $\epsilon_{300,d}K_1$, the slopes, were obtained from least-squares fits at each temperature. The logarithms of these quantities are plotted against $1/T_3$ in Figure 2b. Further least-squares treatments gave eq 8 and eq 9.

$$\ln(\epsilon_{300,d}K_1) = -7648(0.9\%)/T_3 + 17.316(0.7\%) \quad (8)$$

$$\ln(\epsilon_{300,h}K_3) = -1412(1.7\%)/T_3 + 6.118(0.7\%) \quad (9)$$

The standard deviations (shown in parentheses) are surprisingly small in view of the scatter of points (Figure 2a). Values for sample 4, with $(C_b)^{0.5}/C_w = 27$, and one point for sample 7, Y = 626 at 570 K, could not be conveniently included in Figure 2a but were included in the least-squares calculation.

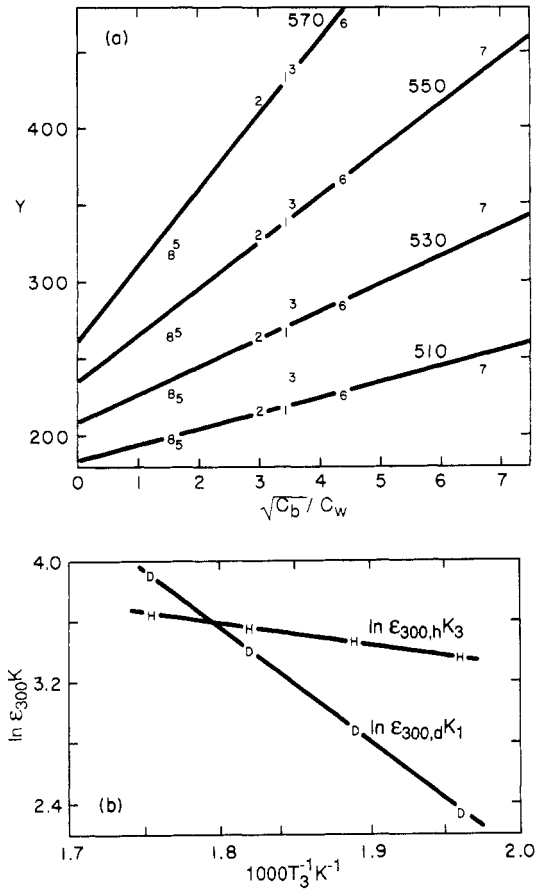

Figure 2. (a) Plots of Y, see eq 7, vs $(C_b)^{0.5}/C_w$ at various temperatures (K). Least-squares lines are shown. Sample numbers (Table I) are used as data point labels. (b) Plots of ln $(\epsilon_{300,d}K_1)$, the least-squares slopes, and ln $(\epsilon_{300,h}K_3)$, the intercepts, from part a, vs $1/T_3$. The lines represent least-squares fits, eq 8 and eq 9, respectively.

In an alternative treatment, eq 10 was derived from results of the preliminary study of $FeBr_2$–Br_2–HBr mixtures, samples 1 and 2. The expected dimer absorbance, $A_{300,d} = \epsilon_{300,d}C_d = \epsilon_{300,d}K_1C_b$,

$$\ln(\epsilon_{300,d}K_1) = -7404(1.1\%)/T_3 + 16.882(0.8\%) \quad (10)$$

in range 2 was then calculated from eq 10 and the hydrate absorbance, $A_{300,h}$, taken as $A_{300,dh} - A_{300,d}$. On this basis the separate absorbances for hydrate, dimer, and monomer, respectively, are listed for each of the 62 observations in Table II (supplementary material). Values of $\epsilon_{300,h}K_3 = \epsilon_{300,h}C_h/C_w(C_bRT_1)^{0.5}$ were derived at each temperature; see Figure 3. A least-squares treatment of ln $\epsilon_{300,h}K_3$ versus $1/T_3$ gave eq 11, shown as the line in Figure 3. The constants in eq 9 and eq 11 do not differ beyond experimental uncertainty. The fit was not quite as good when eq 8 was used instead of eq 10. Because eq 10 was derived from data from less complex mixtures, it was used rather than eq 8. In a parallel treatment, data did not correlate as well when the hydrate was assumed to be $Fe_2(H_2O)Br_6$ and standard deviations were not improved noticeably by inclusion of small amounts of dimer hydrate.

$$\ln(\epsilon_{300,h}K_3) = -1400(3.2\%)/T_3 + 6.070(1.4\%) \quad (11)$$

Formula of the Hydrate Vapor Molecule. It should be emphasized that, in addition to $Fe(H_2O)Br_3(g)$, the concentration of any vapor molecule with formula $Fe_x(H_2O)Br_{2x+1}$, with x an integer, will, in range 2, also be proportional to the product $C_wC_b^{1/2}$. Hence the extra absorbance must be assumed to include contributions from all such molecules. However, it seems unlikely that mixed-valence polymers make a significant contribution.[6] If, for example, $\Delta G°$ for the dissociation of the simple mixed-valence dimer Fe_2Br_5, i.e. $Fe_2Br_5 = FeBr_2 + FeBr_3$, is assumed to be the

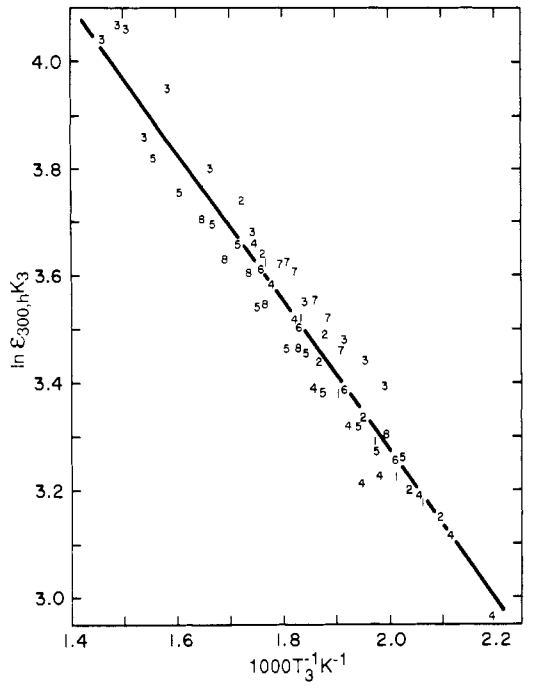

Figure 3. Values of ln ($\epsilon_{300,h}K_3$), calculated from data in Table II (supplementary material), at various temperatures in range 2. Sample numbers (Table I) are used as data point labels. The line represents the least-squares fit, eq 11.

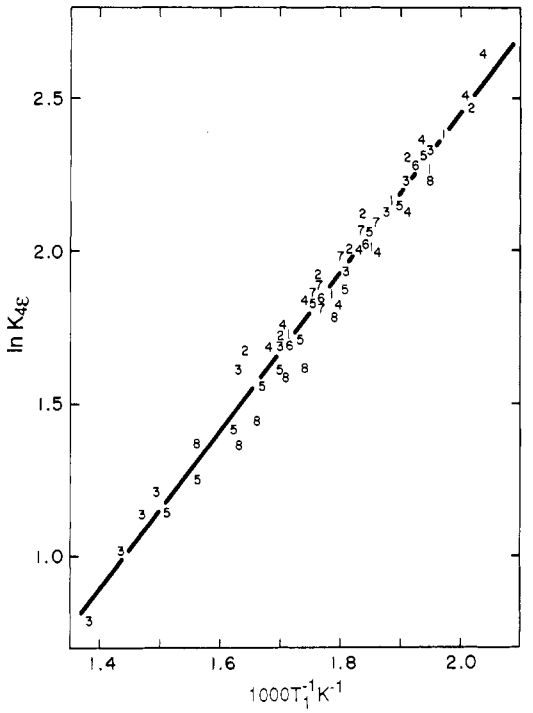

Figure 4. Values of ln $K_{4\epsilon}$, calculated from data in Table II (supplementary material), at various temperatures in range 2. Sample numbers (Table I) are used as data point labels. The line represents the least-squares fit, eq 12.

mean of values for $Fe_2Br_6 = 2FeBr_3$ and $Fe_2Br_4 = 2FeBr_2$, the concentration of Fe_2Br_5 may be estimated. Because the vapor pressure of $FeBr_2(s)$ is very low in range 2, such an estimate projects a concentration of Fe_2Br_5 only a few percent or less of $FeBr_3$. Hence it has been assumed that, similar to the result found in the chloride system,[2] $Fe(H_2O)Br_3(g)$ is the dominant hydrate vapor species.

Absorbances in Ranges 1 and 3. The absorbance contributions of the various molecules in ranges 1 and 3 were calculated as follows. The dimer and hydrate contributions were assumed related by $K_{4\epsilon}$, the equilibrium constant for reaction 4. $K_{4\epsilon} \equiv$ $\epsilon_{300,h}C_h/C_w(\epsilon_{300,d}C_dRT_1)^{0.5}$. First values of $K_{4\epsilon}$ were derived by using results listed in Table II (supplementary material) for range 2. A least-squares treatment of these gave eq 12, see also Figure 4. Equation 12 was then extrapolated to obtain values of $K_{4\epsilon}$ at temperatures in ranges 1 and 3. The dimer and monomer contributions were assumed to be related by the monomer–dimer equilibrium constant $K_{md\epsilon}$, $\epsilon_{300,m}K_2/(\epsilon_{300,d}K_1)^{0.5}$. $K_{md\epsilon}$ values were derived from $\epsilon_{300,m}$, eq 6 and eq 10, giving eq 13. With these substitutions, eq 5 was then used to calculate the contribution of each component in ranges 1 and 3.

$$\ln K_{4\epsilon} = 2596(2.2\%)/T_1 - 2.742(3.7\%) \quad (12)$$

$$\ln K_{md\epsilon} = -8711/T_1 + 11.912 \quad (13)$$

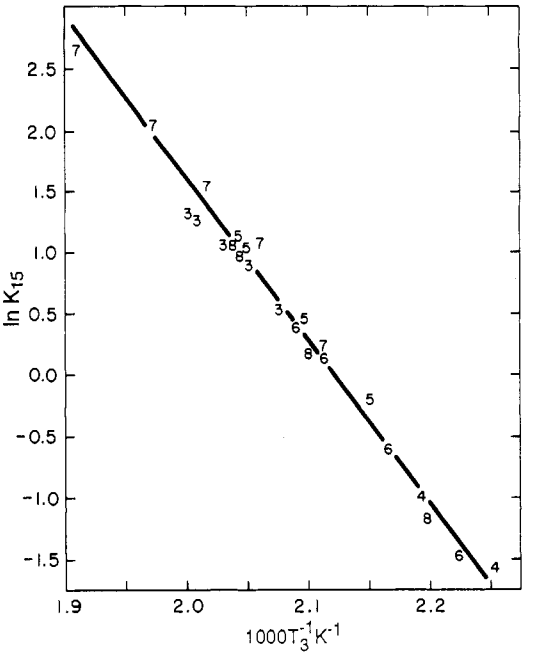

Figure 5. Values of ln K_{15}, calculated from data in Table II (supplementary material), at various temperatures in range 1. Sample numbers (Table I) are used as data point labels. The line represents the least-squares fit, eq 15.

Table IV. Constants Derived for Equations of the Form $R_\lambda = a + bT$ at Various Wavelengths, λ, and Values of R_λ for the Monomer[a]

	$Fe(H_2O)Br_3$		Fe_2Br_6		$FeBr_3$
λ, nm	a	10^3b, K^{-1}	a	10^3b, K^{-1}	R_λ
320	0.591	0.518	0.907	0.160	1.03
340	0.172	0.862	0.513	0.393	0.824
360	0.109	0.872	0.111	0.805	0.747
380	0.412	0.525	0.054	0.806	0.921
400	0.960	−0.288	0.033	0.912	1.321
420	1.526	−0.686	1.090	−0.370	2.056
440	1.303	−0.208	1.105	−0.202	2.154
460	0.719	0.435	1.507	−0.767	2.054
480	0.138	0.999	1.097	−0.342	1.642

[a] Empirical least-squares fit for the temperature range 490–720 K.

Behavior When a Condensed Hydrate Phase Is Present. The hydrate contribution to the absorbance in range 1, see Table II (supplementary material), where the vapor is believed to be in equilibrium with a condensed hydrate phase, shows a systematic dependence on the concentration of water vapor. This would not be expected if the condensed phase (cp) were $Fe(H_2O)Br_3(cp)$. As found in the chloride system,[2] the calculated hydrate absorbances for the various samples correlate reasonably well, assuming an equilibrium constant of the form expected for reaction 14, $\epsilon_{300,h}K_{14} = \epsilon_{300,h}C_hRT_1(C_wRT_1)^{0.5}$. (As noted previously[2] the formula $Fe(H_2O)_{1.5}Br_3$ is empirically equivalent to the combination $Fe(H_2O)_6^{3+} + 3FeBr_4^-$, or alternatively, $Fe_2Br_6(H_2O)_3$.)[9,10] A

$$Fe(H_2O)_{1.5}Br_3(cp) = Fe(H_2O)Br_3(g) + 0.5H_2O(g) \quad (14)$$

Table V. Thermodynamic Constants for Bromide and Chloride Reactions in the Vicinity of 600 K

		bromide		chloride		ref
reacn	eq	$\Delta H°$, kJ mol^{-1}	$\Delta S°$, J K^{-1} mol^{-1}	$\Delta H°$, kJ mol^{-1}	$\Delta S°$, J K^{-1} mol^{-1}	(chloride)
1	10	61.56	64.12	25.88	69.57	13
3	11	11.64	−20.18	−8.36	−15.01	2, 13
4	12	−21.58	−55.32	−21.30	−49.80	2
14	15	108.88	160.34	99.40	141.5	2
16	17	93.55	171.43	107.76	156.5	2, 13
22	11, 6	−91.6	−124	−93.6	−121	2
22	12, 13	−94.0	−127			

	bromide		chloride		ref
T, K	$\Delta H°_f$, kJ mol^{-1}	$S°$, J K^{-1} mol^{-1}	$\Delta H°_f$, kJ mol^{-1}	$S°$, J K^{-1} mol^{-1}	(chloride)
500	−508	502	−590	471	2

plot of ln K_{15}, $K_{15} = \epsilon_{300,h}K_{14}$, vs $1/T_3$ is shown in Figure 5. The least-squares lines corresponds to eq 15. The fit is less satisfactory,

$$\ln K_{15} = -13096(2.4\%)/T_3 + 27.782(2.4\%) \quad (15)$$

with standard deviations more than twice larger, if the condensed phase is assumed to be $Fe(H_2O)Br_3$.

From the proposed reactions, $FeBr_2(s)$ and $Fe(H_2O)_{1.5}Br_3(cp)$ should be in equilibrium for each sample at the temperature at which ranges 1 and 2 intersect, $T_{1,2}$; see Figure 1 and Table I. The equilibrium constant for reaction 16 is fixed by C_w and C_b;

$$Fe(H_2O)_{1.5}Br_3(cp) = FeBr_2(s) + 0.5Br_2(g) + 1.5H_2O(g) \quad (16)$$

the absorbance is only needed to find $T_{1,2}$. A least-squares treatment of ln K_{16} = ln $(C_b/C_w)^{0.5}(C_wRT_{1,2})^2$ versus the $1/T_{1,2}$ values observed for the various samples gave eq 17. The constants

$$\ln K_{16} = -11252(3.2\%)/T_{1,2} + 20.62(3.6\%) \quad (17)$$

in eq 17 compare favorably with those calculated for this reaction from absorbance data, i.e. eq 15–eq 11, −11696 and 21.71.

Support for the composition proposed for the condensed hydrate phase is also found in results of an earlier study in which total gas pressures generated by four different mixtures of Fe_2O_3 and HBr were measured.[11,12] At low temperatures, a condensed hydrate phase was present and total pressures, P_t, were found to be independent of the amount of HBr added. A least-squares treatment of ln P_t vs $1/T$ for all four samples in the range 400–480 K gives the result ln $P_t = -5642(0.82\%)/T + 10.97(0.94\%)$. If, as suggested from the present work, the condensed hydrate phase is $Fe_2(H_2O)_3Br_6(cp)$ and $Fe_2O_3(s)$ is present, the HBr pressure would be fixed by equilibrium 18. Similarly, with $FeBr_2(s)$ also

$$Fe_2(H_2O)_3Br_6(cp) = Fe_2O_3(s) + 6HBr(g) \quad (18)$$

present, the partial pressures of Br_2 and H_2O would be fixed by eq 16. If it is assumed that $P_w = 3P_b$, eq 17 may be used to find P_w and P_b. The equilibrium constant for eq 18 and hence the partial pressure of HBr may be calculated from $\epsilon_{300,h}K_{14}$, eq 15, $\epsilon_{300,h}K_3$, eq 11, and K_{19}, evaluated from thermodynamic data from the literature for reaction 19.[13] K_{18} is equal to $(K_{14}/K_3)^2/K_{19}$.

$$Fe_2O_3(s) + 6HBr(g) = 2FeBr_2(s) + Br_2(g) + 3H_2O(g) \quad (19)$$

With three condensed phases present, the partial pressures of HBr, Br_2, and H_2O, respectively, would then be fixed at a given temperature, and the total pressure would be independent of the starting ratio of Fe_2O_3 and HBr. The iron(III) bromide vapor molecules do not contribute measurably to the total pressure between 400 and 480 K. On this basis the total pressures predicted from the absorbance data are given by the equation ln $P_t = -5692/T + 11.08$, which agrees, within experimental uncertainty, with the result observed by MacLaren.[11] One does not expect ln P_t, with P_t the sum of the three partial pressures, to be a true linear function of $1/T$. However, the contribution of HBr is, for these samples, less than 7% of P_t in the temperature range where the condensed hydrate phase is present. Hence P_t closely approximates $4P_b$. With $P_w = 3P_b$, eq 17 gives ln $(4P_b) = -5626/T + 10.87$.

Absorbances between 300 and 480 nm. Absorbances of the various samples were measured at 20 nm intervals in the range 300–480 nm. In some cases values exceeded the limit of the instrument or were too small to be measured with reasonable accuracy. In all, however, 707 additional observations (Table III, supplementary material) were examined to see if they were compatible with conclusions based on range 2 at 300 nm. At each wavelength, λ, data were compared in the form of eq 20. In eq

$$A_\lambda - A_{\lambda,b} = R_{\lambda,h}\epsilon_{300,h}C_h + R_{\lambda,d}\epsilon_{300,d}C_d + R_{\lambda,m}\epsilon_{300,m}C_m \quad (20)$$

20, $R_{\lambda,h} = \epsilon_{\lambda,h}/\epsilon_{300,h} = a_h + b_hT_1$, $R_{\lambda,d} = \epsilon_{\lambda,d}/\epsilon_{300,d} = a_d + b_dT_1$, and $R_{\lambda,m} = \epsilon_{\lambda,m}/\epsilon_{300,m}$. A least-squares treatment was used to derive values for the five assumed constants a_h, b_h, a_d, b_d, and $R_{\lambda,m}$. The b constants were introduced to provide an empirical approximation for the temperature dependence of the absorptivities of the hydrate and the dimer. A b term for the monomer was not included since its contribution is very small except at the highest temperatures. The constants derived are shown in Table IV. These equations were used with eq 20 to calculate the expected absorbance, A_{calc}, which was then compared with A_{obs}. The average (absolute) deviation of $(A_{obs} - A_{calc})100/A_{obs}$ for the 707 observations was 3.2%. The maximum deviation of $(A_{obs} - A_{calc})$ × path length was 0.036. Only five deviations were greater than 0.025, the estimated combined uncertainty of readings of the observed absorbance, the base line, and the bromine contribution. Bromine contributes a major part of the absorbance at wavelengths around its absorption maximum, 420 nm. The good overall fit is taken as evidence that the bromine concentrations were evaluated correctly.

Molar Absorptivities and Thermodynamic Properties. A value for the molar absorptivity of the hydrate at 300 nm was derived from data in range 3. If all the iron is in the vapor phase, C_h is given by eq 21. Absorptivities from earlier work[6], $\epsilon_{300,d} = 9600$

$$C_h = C_0(Fe) - 2C_d - C_m = \epsilon_{300,h}C_h/\epsilon_{300,h} \quad (21)$$

and $\epsilon_{300,m} = 2570$ M^{-1} cm^{-1}, were used to derive values of C_d and C_m from the calculated values of $\epsilon_{300,d}C_d$ and $\epsilon_{300,m}C_m$ (Table II, supplementary material). A least-squares treatment of $2C_d + C_m$ vs $\epsilon_{300,h}C_h$ for each sample was then used to derive values of $C_0(Fe)$ and $\epsilon_{300,h}$. The results for $C_0(Fe)$, $C_0(Fe)$ (spec) in Table I, compare favorably with the analytical results. Values of $\epsilon_{300,h}$, in each case a mean for the temperatures of range 3, were (sample no.) as follows: (4) 4899, (6) 5029, (7) 4851, and (8) 4250 M^{-1} cm^{-1}; average 4760 (standard deviation 350) M^{-1} cm^{-1}. A direct calculation, using analytical values for $C_0(Fe)$, C_d, and C_m calculated as above, gave the following values (sample no.): (4) 4801, (6) 5363, (7) 4658, and (8) 5289 M^{-1} cm^{-1}; average 5028 (standard deviation 350) M^{-1} cm^{-1}. A mean, $\epsilon_{300,h}$ = 4900, along with $\epsilon_{300,d}$ = 9600 and $\epsilon_{300,m}$ = 2570 M^{-1} cm^{-1}, was used, with R values from Table IV, to derive an absorption spectrum between

(9) Asakura, K.; Nomura, M.; Kuroda, H. *Bull. Chem. Soc. Jpn.* **1985**, *58*, 1543–1549.
(10) Magini, M. *J. Chem. Phys.* **1982**, *76*, 1111–1115.
(11) MacLaren, R. O. Ph.D. Thesis, University of Washington, Seattle, WA, 1954.
(12) Christian, J. D.; Gregory, N. W. *J. Phys. Chem.* **1967**, *71*, 1583–1587.

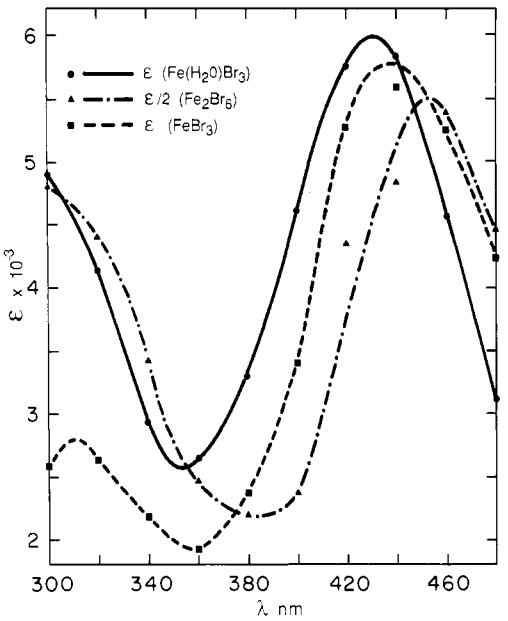

Figure 6. Derived spectra for $Fe(H_2O)Br_3(g)$, $Fe_2Br_6(g)$, and $FeBr_3(g)$, respectively, at 500 K.

300 and 480 nm for each component, the hydrate, the dimer, and the monomer (Figure 6).

Inclusion of various estimates of the temperature dependence of ϵ_{300} values for the dimer and monomer did not significantly reduce the scatter in the result for the hydrate, nor did values of the latter show a systematic trend with temperature. As seen in Figure 6, the wavelength range of the observations does not include the entire range of the overlapping absorption bands; a study of the integrated absorptivities over the observed range did not prove useful as a basis for estimating the temperature dependence of the various ϵ_{300} values.

The assigned mean value of $\epsilon_{300,h}$, 4900 M^{-1} cm^{-1}, was used with the least-squares results to calculate thermodynamic constants for the various reactions; see Table V. Previously reported constants for the corresponding reactions in the chloride system are included for comparison. A standard enthalpy of formation and a standard entropy for $Fe(H_2O)Br_3(g)$ at 500 K were derived from $\Delta H°$ and $\Delta S°$, respectively, for the assumed reaction 3 and literature values[13] for $FeBr_2(s)$, $H_2O(g)$, and $Br_2(g)$. An uncertainty of 500 M^{-1} cm^{-1} in $\epsilon_{300,h}$ introduces an uncertainty of 0.9 J K^{-1} mol^{-1} in the entropy. If $\epsilon_{300,h}$ varies significantly with temperature, a correction will be required in the derived enthalpy changes. The overall uncertainties in the derived thermodynamic properties are difficult to estimate, probably several percent.

Enthalpy and entropy changes derived for reaction 22, eq 3 – eq 2, reflect properties of the Fe–OH_2 bond for the assumed hydrate vapor molecule. Values for the chloride and the bromide

$$FeX_3(g) + H_2O(g) = Fe(H_2O)X_3(g) \qquad (22)$$

are very similar (Table V). The difference $S°(Fe(H_2O)Br_3(g)) - S°(Fe(H_2O)Cl_3(g))$, 31 J K^{-1} mol^{-1}, agrees well with that expected from the different masses of the halogen atoms.[14]

Acknowledgment. Helpful discussions with Professor D. S. Rustad are acknowledged with thanks.

Supplementary Material Available: Table II, listing temperatures, calculated contributions of hydrate, dimer, and monomer, respectively, to A_{300}, $(A_{300}(obs) - A_{300}(calc)) \times$ path length, fraction of absorbance contributed by hydrate, ln $(\epsilon_{300,h}K_3)$, ln K_{4e}, C_w, and C_b, and Table III, listing observed absorbances for the various samples at 20-nm intervals, 300–480 nm (4 pages). Ordering information is given on any current masthead page.

(13) Chase, M. W., Jr.; Davies, C. A.; Downey, J. R., Jr.; Frurip, D. J.; McDonald, R. A.; Syverud, A. N. *JANAF Thermochemical Tables*, 3rd ed.; American Chemical Society and American Institute of Physics: New York, 1986.
(14) Lewis, G. N.; Randall, M.; Pitzer, K. S.; Brewer, L. *Thermodynamics*, 2nd ed.; McGraw-Hill: New York, 1961; p 517.

Contribution from the School of Chemistry, University of Sydney, NSW 2006, Australia

Vapor-Phase Infrared Spectrum of Bis(cyclopentadienyl)beryllium

Kerry W. Nugent and James K. Beattie*

Received December 11, 1987

The vapor-phase infrared spectrum of bis(cyclopentadienyl)beryllium has been recorded at room temperature with a FTIR spectrometer. Although the absorption is very weak, two regions of the spectrum can be used to infer structural features of the molecule. The appearance of seven bands above 3000 cm^{-1} in the C–H stretching region excludes highly symmetric ferrocene-like structures and cyclopentadiene-like σ-bonded structures. The similarity of the spectrum in the 1100–700-cm^{-1} region to those of the molecule in condensed phases is further evidence that the slip-sandwich structure of the condensed phases persists in the vapor phase. This conclusion is opposite that reached in an earlier infrared study but is consistent with the conclusions of the most recent electron diffraction investigation.

Introduction

At least four different structures have been proposed for bis(cyclopentadienyl)beryllium ($BeCp_2$), commonly but inappropriately termed "beryllocene". These are illustrated in Figure 1. When first prepared in 1958,[1] the compound was found to be polar with quite large dipole moments of 2.46 D in benzene and 2.24 D in cyclohexane.[2] This excludes the D_{5d} structures of ferrocene and of the homologous compound magnesocene,[3] which are nonpolar. The space group of solid $BeCp_2$ was determined to be $P2_1/c$, however, with two molecules per unit cell.[4] This is isomorphous with ferrocene and means that the structure of $BeCp_2$ in the solid state must be centrosymmetric. It was therefore suggested that the compound might have different structures in the solid and solution states.

The first structural study of the compound was made by vapor-phase electron diffraction in 1964.[5] The data could not be fitted to either of the existing models, and a new model that was consistent with both the electron diffraction data and with the existing knowledge about the compound was proposed. This was the C_{5v} unsymmetrical sandwich model, with two parallel rings, as a ferrocene, but with the beryllium atom much closer to one ring than to the other (Figure 1c). This model could explain the

(1) Fischer, E. O.; Hofmann, H. P. *Chem. Ber.* **1959**, *92*, 482.
(2) Fischer, E. O.; Schreiner, S. *Chem. Ber.* **1959**, *92*, 938.
(3) Bünder, W.; Weiss, E. *J. Organomet. Chem.* **1975**, *92*, 1.
(4) Schneider, R.; Fischer, E. O. *Naturwissenschaften* **1963**, *50*, 349.
(5) Almenningen, A.; Bastiansen, O.; Haaland, A. *J. Chem. Phys.* **1964**, *40*, 3434.

0020-1669/88/1327-4269$01.50/0